Optical properties of stratified systems including lamellar gratings

C. D. Ager and H. P. Hughes
Cavendish Laboratory, Madingley Road, Cambridge CB3 0HE, England
(Received 5 June 1991)

We describe a computational method, based on scattering-matrix techniques, for calculating the electromagnetic response of multilayer systems that may include both anisotropic dielectric media and periodically inhomogeneous grating structures. The method calculates the transmission and reflection coefficients of the structure, the electromagnetic field profiles in any layer, and the dispersion relations for normal modes of the system. As illustrative examples, the method is applied to a silver gratings and to doped semiconductor heterostructures with overlaid metallic gratings that act as photon-plasmon coupling structures.

I. INTRODUCTION

The optical properties of layered systems are of great fundamental and technological importance in a wide range of fields, including semiconductor optoelectronics, thin-film magnetism, and liquid-crystal systems. As the experimental systems become more complex, it is important to be able to model their electromagnetic behavior accurately in order both to optimize the system parameters and to understand the physical processes involved.

Several methods have been used to calculate the electromagnetic properties of multilayer systems, and we begin by reviewing some of the more common ones. The Cartesian axes are chosen as shown in Fig. 1, with the z axis the axis of stratification, and the radiation incident in the x-z plane from the $-z$ direction. Throughout, the harmonic dependence of the electromagnetic (EM) fields in any homogeneous medium is taken as $e^{i(\mathbf{k}\cdot\mathbf{r}-\omega t)}$, where ω is fixed and the wave vector $\mathbf{k}$ depends on the dielectric response of the medium; because ω is constant, the explicit time dependence will be dropped.

The most commonly used method for calculating the optical properties of stratified systems involving homogeneous layers is the transfer-matrix approach pioneered by Abelès,[1] and implementations of this method for anisotropic systems have been given by Teitler and Henvis[2] and Berreman.[3] The lateral homogeneity of the system and the choice of plane of incidence allow the operators

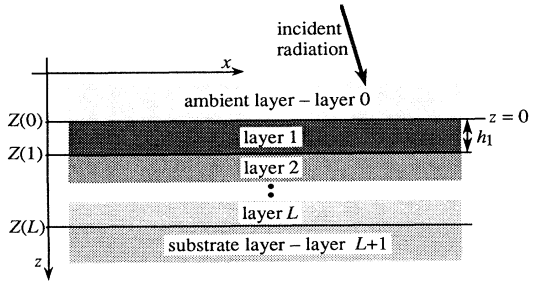

FIG. 1. The coordinate system used for the scattering-matrix calculations. Radiation is incident upon the layered system from $z<0$.

$\partial/\partial y$ and $\partial/\partial x$ to be replaced by 0 and ik_x, respectively. When the constitutive equations are used to substitute for **B** and **D**, Maxwell's equations are simplified to two linear equations and four ordinary differential equations relating the six components of **E** and **H**. The linear equations may be used to eliminate E_z and H_z, leaving four equations that may be expressed in matrix form as

$$\frac{d}{dz}\begin{bmatrix} E_x(z) \\ H_y(z) \\ E_y(z) \\ -H_x(z) \end{bmatrix} = i\omega \underline{P} \begin{bmatrix} E_x(z) \\ H_y(z) \\ E_y(z) \\ -H_x(z) \end{bmatrix}, \tag{1}$$

where $\underline{P}$ is a 4×4 propagation matrix that depends on the x component of the wave vector k_x, the relative dielectric permittivity and magnetic permeability tensors $\epsilon(\omega)$ and $\mu(\omega)$ (spatial dispersion is neglected here), and the optical rotation tensors $\rho(\omega)$ and $\rho'(\omega)$, which describe any optical activity of the medium. The solution of this equation yields a transfer matrix $\underline{T}(z)$, relating the fields at different z within a particularly layer:

$$\begin{bmatrix} E_x(z) \\ H_y(z) \\ E_y(z) \\ -H_x(z) \end{bmatrix} = \underline{T}(z-z_0) \begin{bmatrix} E_x(z_0) \\ H_y(z_0) \\ E_y(z_0) \\ -H_x(z_0) \end{bmatrix}. \tag{2}$$

All the field components related by $\underline{T}$ are tangential to the interfaces between layers, and so are conserved across them. Therefore, an effective transfer matrix for the whole system may be found by multiplying together the transfer matrices for each layer.

Equation (1) can be solved either directly by integration or by determining the eigenvectors of the matrix $\underline{P}$. These four (4×1) eigenvectors $\underline{u}_n$ (where $n=1,2,3,4$) correspond to EM eigenmodes (or *characteristic waves)* of the medium of the layer, and each propagates independently of the others according to $\underline{u}_n(z)=\underline{u}_n(z_0)e^{ik_z^n(z-z_0)}$. In the simplest case of a linear isotropic homogeneous (LIH) medium, the four eigenvectors can be identified as the two plane polarized waves, each propagating towards either $z=+\infty$ or $-\infty$. The eigenvectors give the

transfer matrix $\underline{T}$ immediately from the relation $\underline{T}(z-z_0)=\underline{U}\underline{K}(z-z_0)\underline{U}^{-1}$, where $\underline{U}$ is a matrix, the nth column of which is $\underline{u}_n$, and $\underline{K}(z-z_0)$ is a diagonal matrix with elements $K_{nn}(z-z_0)=e^{ik_z^n(z-z_0)}$, which thus describes the propagation of each eigenmode through the layer.

The transfer-matrix method is generally computationally efficient, stable, and simple to implement, but fails to give accurate results in some cases. In particular, if the EM eigenmodes are evanescent in a layer, the fields of the modes that decay away from an interface (towards $z=+\infty$) will tend to be masked by the modes that are decaying "backwards" (i.e., towards $z=-\infty$) from the next interface. The transfer-matrix method fails to give stable results if the number or depth of layers in which the modes decay exceeds a limit imposed by the numerical precision of the computer used for the calculations. For systems with a grating, the higher diffracted orders decay in every layer, and the transfer-matrix approach fails except for the case of a simple grating on a homogeneous substrate.

An alternative method is the scattering-matrix technique described by Ko and Inkson and Ko and Sambles[4] (an equivalent method has recently been given by Chew[5]). This technique maintains a distinction between the forward- and backward-traveling modes in each layer, and thus avoids the numerical instability that occurs for the transfer-matrix method. The scattering-matrix technique is described in detail in Sec. II.

The electromagnetic theory of gratings has been reviewed by Petit,[6] who describes four classes of method that are applicable to a variety of grating calculations:

(1) The Rayleigh method: this assumes that the total EM field above a perfectly conducting corrugated surface can be expressed as a Fourier series, where the Fourier coefficients are determined by applying the boundary conditions along the surface. The method is generally successful, provided that the grating grooves are shallow compared to the period and the wavelength of the radiation.

(2) Modal-expansion methods: for certain grating profiles, it is possible to calculate a modal expansion of the fields in the grooved region, which can be matched to the Fourier components of the diffracted field outside the grating, giving an approximate a solution if the series is terminated. In fact, it has recently been shown[7] that a modal expansion may be used for lamellar gratings without the restriction to perfectly conducting metals, and, furthermore, that this method is not restricted to gratings with shallow grooves.

(3) Integral methods: the first rigorous methods used to calculate diffraction by a perfectly conducting grating were the integral methods proposed by several authors (e.g., Ref. 8). These methods rely on the fact that the diffracted fields can be expressed exactly as integrals of the surface current density on the grating. The current is found by using the integral expressions for the field at the grating surface and applying the boundary conditions, leading to an integral equation of the first kind, which can be solved approximately by various numerical techniques. Although the integral methods were originally applied only to perfectly conducting gratings, the method has been extended to metallic gratings by generalizing the function that describes the surface current on the grating. In these cases, a set of coupled integral equations is found that must be solved simultaneously.

(4) Differential methods: the fourth approach uses one of several differential methods, and differs from the others in that it was originated in an attempt to deal with dielectric and metallic gratings rather than the perfectly conducting case. The direct solution of the coupled partial differential equations that constitute Maxwell's equations is possible, but is very time consuming and is only numerically stable for weakly modulated gratings. The solution is simpler if the fields of Maxwell's equations are projected onto an exponential basis via the Fourier transform. The resulting equations are coupled ordinary differential equations and the unknowns are functions of just one variable, so numerically efficient techniques such as the Runge-Kutta algorithm may be used. A conformal mapping of the grating can be used to replace the grating profile with a plane before proceeding as above; this technique also allows the perfectly conducting case to be solved by the differential method.

The next section describes the scattering-matrix method as it applies to systems of laterally homogeneous layers. This method is then modified in Sec. III to allow the inclusion of layers that are periodically inhomogeneous. In particular, it is shown that a modal expansion [method (2) above] of the grating fields can be used in the scattering-matrix method to model a lamellar grating on a stratified substrate. Modal expansions can be derived particularly easily for the case of a perfectly conducting grating, and a numerical approximation can be obtained for the case of a metallic or dielectric grating.[7] Section IV then presents some examples of calculations of the optical properties of diffraction gratings on multilayer substrates in the visible and far-infrared frequency ranges.

While the scattering-matrix approach is applied here to systems of electromagnetic interest, it should be noted that it also has considerable application in situations involving quantum-mechanical waves, such as resonant tunneling (e.g., Ref. 4) and the dynamics of electrons in microstructured solid-state devices.

II. THE SCATTERING-MATRIX APPROACH FOR LATERALLY HOMOGENEOUS MULTILAYER SYSTEMS

The scattering matrix $\underline{S}(0,L+1)$ of a system consisting of L homogeneous layers between substrate (layer $L+1$) and ambient (layer 0) media relates the amplitudes of the *scattered* eigenmodes to the amplitudes of the modes that are *incident* upon the system:

$$\begin{bmatrix} \underline{a}_{L+1} \\ \underline{b}_0 \end{bmatrix} = \underline{S}(0,L+1) \begin{bmatrix} \underline{a}_0 \\ \underline{b}_{L+1} \end{bmatrix} = \begin{bmatrix} \underline{S}_{11}(0,L+1) & \underline{S}_{12}(0,L+1) \\ \underline{S}_{21}(0,L+1) & \underline{S}_{22}(0,L+1) \end{bmatrix} \begin{bmatrix} \underline{a}_0 \\ \underline{b}_{L+1} \end{bmatrix} . \quad (3)$$

Here the elements of the (2×1) vector $\underline{a}_0$ are the coefficients of the modes incident upon the system from the ambient medium, $\underline{b}_0$ represents the reflected modes in the ambient layer and $\underline{a}_{L+1}$ the transmitted modes in the substrate. $\underline{b}_{L+1}$ contains the coefficients of the modes incident from the substrate layer, and is generally set to $\underline{0}$ when modeling an experimental system where the light is incident only from the ambient side. The 4×4 matrix $\underline{S}$ may be split into the four 2×2 "quarter" submatrices as shown in (3), and this decomposition is required in the following algorithm, first given by Ko and Inkson and Ko and Sambles.[4]

The scattering matrix is constructed from the layer matrices $\underline{L}_l$, defined by

$$\begin{bmatrix}\underline{a}_l\\ \underline{b}_l\end{bmatrix}=\underline{L}_l\begin{bmatrix}\underline{a}_{l+1}\\ \underline{b}_{l+1}\end{bmatrix}. \tag{4}$$

(Note that the term "layer matrix" is used here rather than "interface matrix" as used in Ref. 4 because $\underline{L}_l$ includes the propagation of the modes through a layer.) $\underline{L}_l$ relates the coefficients of the modes in one layer to those in the next layer, and in that sense is analogous to the transfer matrix characterizing layer l, $\underline{T}_l$. Once the eigenmodes of the two layers have been determined, the EM boundary conditions will relate the coefficients of these modes at the interface, and these conditions are embodied by (4). The calculation of the scattering matrix from the layer matrices is quite independent of the exact form of the modes (hence the ease with which the same formalism can be used to describe both optical properties, as here, and electron-transport phenomena, as in Ref. 4).

Assume the scattering matrix for a system of l layers $\underline{S}(0,l)$ has been found, and another layer is added to the system. The equation for $\underline{L}_l$, (4), and the equations defining $\underline{S}(0,l)$ and $\underline{S}(0,l+1)$, (3), may then be solved for $\underline{S}(0,l+1)$, giving[4]

$$\begin{aligned}
\underline{S}_{11}(0,l+1)&=(\underline{L}_{11}-\underline{S}_{12}\underline{L}_{21})^{-1}\underline{S}_{11}\ ,\\
\underline{S}_{12}(0,l+1)&=(\underline{L}_{11}-\underline{S}_{12}\underline{L}_{21})^{-1}(\underline{S}_{12}\underline{L}_{22}-\underline{L}_{12})\ ,\\
\underline{S}_{21}(0,l+1)&=\underline{S}_{22}\underline{L}_{21}\underline{S}_{11}(0,l+1)+\underline{S}_{21}\ ,\\
\underline{S}_{22}(0,l+1)&=\underline{S}_{22}\underline{L}_{21}\underline{S}_{12}(0,l+1)+\underline{S}_{22}\underline{L}_{22}\ ,
\end{aligned} \tag{5}$$

where the subscripts refer to the four "quarter" submatrices as in (3), and, unless explicitly stated otherwise, the $\underline{S}_{ij}$ and $\underline{L}_{ij}$ submatrices on the right-hand side refer to $\underline{S}(0,l)$ and $\underline{L}_l$, respectively. The calculation begins by taking $\underline{S}(0,0)$ as the identity matrix $\underline{1}$. New layers are added to the system and the new scattering matrix is determined by (5) until all $L+1$ layers have been included and the scattering matrix for the entire system has been found.

When the dielectric tensor contains no off-diagonal elements, $\underline{P}$ becomes 2×2 block diagonal. Each 2×2 submatrix represents one of the two plane polarizations (s and p), which cannot interact and are good eigenmodes in this limited class of anisotropic systems. If each polarization is treated separately (i.e., only two eigenmodes—one polarization, forward and backward—are considered instead of four), the layer matrices for a laterally homogeneous system are then all of order 2×2 instead of 4×4, and the corresponding eigenvectors u_n have as elements only either E_x and H_y for p polarization, or E_y and H_x for s polarization, and the coefficients of the modes in layer l, a_l and b_l, are now scalar quantities. Since this leads to a considerable saving of computation time without placing unreasonable restrictions on the systems that may be modeled, the 2×2 system will be adopted unless otherwise stated. Only p polarization will be considered explicitly; the equivalent expressions for s polarization may be derived following the same arguments but substituting E_y and $-H_x$ for E_x and H_y, respectively.

As the eigenmodes propagate from one layer (l) to the next ($l+1$), the electromagnetic boundary conditions must be satisfied by the sum of the fields of the eigenmodes. The elements of $\underline{u}_n$ are the components of **E** and **H** parallel to the interface, so each element must be conserved across the boundary. Thus the electromagnetic boundary condition for E_x requires

$$\begin{aligned}
a_l E_l^{(+)}e^{ik_z(l)h_l}+b_l E_l^{(-)}=a_{l+1}E_{l+1}^{(+)}+b_{l+1}E_{l+1}^{(-)}\\
\times e^{-ik_z(l+1)h_{l+1}}\ ,
\end{aligned} \tag{6}$$

where $E_l^{(\pm)}$ represents the x component of the electric field in the lth layer at the boundary from which the mode propagates or decays and where $k_z(l)$ is the z component of the wave vector in layer l. $(+)$ indicates a forward mode and $(-)$ a backward mode in the layer. Referring to Fig. 2, the boundary condition in (6) is applied at the interface between points A and B, but $E_l^{(+)}$ and $E_{l+1}^{(-)}$ represent the E_x field at points C and D, respectively, and the exponential terms in (6) represent the phase shift or decay of these modes each within the appropriate layer to points A and B.

The full boundary conditions may be expressed as a matrix equation as follows:

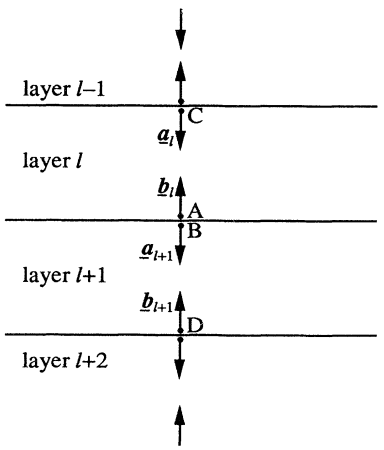

FIG. 2. Field matching at the interface between layers l and $l+1$: the boundary conditions require that E_x and H_y are conserved between points A and B. $\underline{a}_l$ and $\underline{b}_{l+1}$ are defined at C and D, respectively, so the contribution of these modes to the fields at the $l:l+1$ interface is given by the values at C and D multiplied by an appropriate phase factor, as shown in Eq. (6).

$$\begin{bmatrix} E_l^{(+)} & E_l^{(-)} \\ H_l^{(+)} & H_l^{(-)} \end{bmatrix} \begin{bmatrix} e^{ik_z(l)h_l} & 0 \\ 0 & 1 \end{bmatrix} \begin{bmatrix} a_l \\ b_l \end{bmatrix} = \begin{bmatrix} E_{l+1}^{(+)} & E_{l+1}^{(-)} \\ H_{l+1}^{(+)} & H_{l+1}^{(-)} \end{bmatrix} \begin{bmatrix} 1 & 0 \\ 0 & e^{-ik_z(l+1)h_{l+1}} \end{bmatrix} \begin{bmatrix} a_{l+1} \\ b_{l+1} \end{bmatrix} . \quad (7)$$

(7) may also be written as

$$\underline{U}_l \underline{K}_l^{+} \begin{bmatrix} a_l \\ b_l \end{bmatrix} = \underline{U}_{l+1} \underline{K}_{l+1}^{-} \begin{bmatrix} a_{l+1} \\ b_{l+1} \end{bmatrix} . \quad (8)$$

It is now clear that the layer matrix, defined by (4), is given by

$$\underline{L}_l = (\underline{U}_l \underline{K}_l^{+})^{-1} (\underline{U}_{l+1} \underline{K}_{l+1}^{-}) . \quad (9)$$

As in Sec. I, $\underline{U}$ and $\underline{K}^{\pm}$ are constructed from the eigenmodes of layer l and their associated k_z^n. The eigenmodes

$$\underline{u}_n(l) = \begin{bmatrix} E_l^{(\pm)} \\ H_l^{(\pm)} \end{bmatrix}$$

and $k_z^n(l)$ may in turn be calculated as described in Sec. I by finding the eigenvectors of the matrix $\underline{P}$ in Eq. (1).

In Sec. III, this method is adapted to allow the inclusion of layers that are periodically inhomogeneous.

III. THE SCATTERING-MATRIX APPROACH FOR SYSTEMS INCLUDING GRATINGS

The scattering-matrix method may be extended to allow the inclusion of layers that are periodically inhomogeneous in the x direction. If such a layer is present in a system, it is no longer true that k_x must be conserved throughout the system; if the lateral modulation has period d, modes with k_x differing by $2\pi/d$ can interact in the modulated layer. A single incident mode thus produces an infinite number of scattered modes, each with wave vector k^n, the x component of which is given by

$$k_x^n = k_{0x} + n\frac{2\pi}{d} , \quad (10)$$

where k_{0x} is the x component of the incident wave vector k_0. Each value of n corresponds to a distinct diffracted order, and each order corresponds to two eigenmodes within a layer (forward and backward) for a given polarization state. In an isotropic medium of dielectric constant ϵ, the propagation of the nth-order modes is described by the z component of the wave vector k^n, given by

$$k_z^n = \pm \left[\epsilon \left[\frac{\omega}{c} \right]^2 - (k_x^n)^2 \right]^{1/2} . \quad (11)$$

The lowest-order modes propagate away from the modulated layer, but as n increases above some critical value, k_z^n rapidly becomes large and imaginary, indicating that the modes are evanescent. The choice of sign in (11) depends on whether the mode is classified as forward or backward. Analytically, the scattered fields are represented by an expansion in terms of these diffracted orders, which may be approximated by a finite number of terms (larger than the critical value of n) because the higher evanescent orders decay away from the modulated layer more rapidly than the lower evanescent orders.

Since the scattered field distribution can be approximated using a finite number of diffracted orders, a matrix formalism analogous to the 2×2 scattering matrix method presented in Sec. II may be constructed, using matrices of order $2M \times 2M$ if M diffracted orders are retained in the calculation. At the boundary between two homogeneous layers, modes of different orders cannot interact because they differ in k_x, so the layer matrix $\underline{L}$ representing the field matching at this boundary is effectively block diagonal, and each 2×2 submatrix can be found exactly as for the standard 2×2 scattering-matrix method. However, at the boundaries of any modulated layer, the translational invariance no longer holds, and eigenmodes with k_x^n with different n may interact. The boundary conditions apply at every point along the interface, so the matching of the tangential fields requires knowledge of the spatial dependence of the eigenmodes in the modulated layer.

Here, it is assumed that the modulated layer is a lamellar diffraction grating. Of the techniques that can be applied to the diffraction problem for this system, the one that fits most naturally with the scattering-matrix method is the modal-expansion method, because this method uses noninteracting eigenmodes in the grooved region. It may be possible to treat more general grating profiles by stacking lamellar gratings with the same period but different mark-to-space ratios and various thicknesses, but this has not yet been attempted. A similar stacking method has recently been used to calculate the radiation characteristics of dielectric gratings of various profiles using a transmission line approach.[9]

A. The eigenmodes of a lamellar grating

For the case of a perfectly conducting lamellar grating, the EM fields may be found quite easily from Maxwell's equations and the condition that the electric field must be zero everywhere in the metal (see, for example, Ref. 7). The more general case of a lamellar grating with period d and mark fraction r, as illustrated in Fig. 3, where each grating finger is composed of an isotropic medium with (complex) relative dielectric constant ϵ, has been considered by Sheng.[7] The method relies on determining k_z for each mode by solving the dispersion relation for that mode numerically. An analytical expression may then be found for each eigenmode in terms of this k_z.

Following Sheng, the values of E_z and H_y may be related at the various *vertical* (i.e., x = const) interfaces through the grating using 2×2 transfer matrices $\underline{T}$:

$$\begin{bmatrix} E_z \\ H_y \end{bmatrix}_{-rd/2} = \underline{T}_1 \begin{bmatrix} E_z \\ H_y \end{bmatrix}_{rd/2} , \qquad \begin{bmatrix} E_z \\ H_y \end{bmatrix}_{rd/2} = \underline{T}_2 \begin{bmatrix} E_z \\ H_y \end{bmatrix}_{(1-r/2)d} . \quad (12)$$

The solution is completed by imposing periodic boundary conditions on the fields, ensuring that the phase change

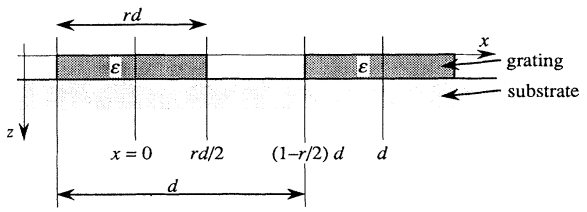

FIG. 3. Dimensions of the grating as used in the calculation. d is the grating period and r is the mark fraction, i.e., the fraction of the period occupied by the material of dielectric constant ϵ.

across one period matches that of the incident mode:

$$\begin{bmatrix} E_z \\ H_y \end{bmatrix}_{(1-r/2)d} = e^{ik_{0x}d} \begin{bmatrix} E_z \\ H_y \end{bmatrix}_{-rd/2} , \tag{13}$$

where $k_{0x}d$ is the phase change of the incident mode across one period. An eigenvalue equation for k_z (k_z is contained in the matrices $\underline{T}_1$ and $\underline{T}_2$) is obtained by combining (32) and (33):

$$|\underline{T}_1\underline{T}_2 - e^{-ik_{0x}d}\underline{1}| = 0 ,$$

where $\underline{1}$ is the identity matrix. After some algebraic simplification, this equation becomes (see also Ref. 10 for other equivalent formulations)

$$\cos(k_{0x}d) - \cos(\beta rd)\cos[\alpha(1-r)d] + \tfrac{1}{2}(\epsilon\alpha/\beta + \beta/\epsilon\alpha)\sin(\beta rd)\sin[\alpha(1-r)d] = 0 , \tag{14}$$

where α and β are given by

$$\alpha^2 = k_0^2 - k_z^2 ,$$
$$\beta^2 = \epsilon k_0^2 - k_z^2 . \tag{15}$$

$$\underline{U} = \begin{bmatrix} E_l^{0(+)} & 0 & 0 & E_l^{0(-)} & 0 & 0 \\ H_l^{0(+)} & 0 & 0 & H_l^{0(-)} & 0 & 0 \\ 0 & E_l^{-1(+)} & 0 & 0 & E_l^{-1(-)} & 0 \\ 0 & H_l^{-1(+)} & 0 & 0 & H_l^{-1(-)} & 0 \\ 0 & 0 & E_l^{+1(+)} & 0 & 0 & E_l^{+1(-)} \\ 0 & 0 & H_l^{+1(+)} & 0 & 0 & H_l^{+1(-)} \end{bmatrix} . \tag{16}$$

If this matrix is combined with an equivalent analogy of $\underline{K}$ in (8), the calculation of $\underline{L}$ will follow exactly the same course as the 2×2 case, and the expression for $\underline{L}$ given in (9) will remain valid. Note that the each layer now supports several independent forward- and backward-traveling modes, so the coefficients $\underline{a}_l$ and $\underline{b}_l$ must be vector quantities.

C. The grating-layer–homogeneous-layer interface

The boundary conditions must hold for all x along the interface, so the equation expressing them now becomes

[cf. (6)]

$$\sum_n [a_l^n E_l^{n(+)}(x) e^{ik_z^{n(l)}h_l} + b_l^n E_l^{n(-)}(x)] = \sum_m [a_g^m E_g^{m(+)}(x) + b_g^m E_g^{m(-)}(x) e^{-ik_z^{n(g)}h_g}] , \tag{17}$$

where the x dependence of the fields has been included explicitly. Layer l is taken as the homogeneous layer, and layer g is the grating. Equation (17) holds over all x

The solution of (14) for k_z gives the dispersion relation for the eigenmodes of the grating. In general, no analytical solution exists, so standard numerical techniques must be used. The most easily applicable method is a simple extension of the Newton-Raphson method[11] to the complex plane. Once k_z has been determined, (12) and (13) may be solved for $E_x(x)$ and $H_y(x)$, and the solution has been given in Ref. 7.

B. Homogeneous layers in systems with gratings

Each diffracted order of a grating produces two new eigenmodes in the homogeneous layers of the system—one forward, one backward (s and p polarizations are not mixed by the grating, so they may still be regarded as independent and treated separately). Each member of the pair of eigenmodes has the same k_x^n, but k_z^n of opposite sign to the other member.

The layer matrix $\underline{L}$ can be found for two adjacent homogeneous layers using an expression similar to Eq. (7). Each row of (7) represents the boundary condition being applied to a specific component of the EM field, and each column of the matrix $\underline{U}$ contains the relative contributions of a particular eigenmode to the various field components. An analogous matrix may be constructed for the case including the extra diffracted orders of the grating. The fields of each order match across a boundary independently, so a column of $\underline{U}$ will contain only two nonzero elements. For example, if only the lowest three orders of the grating (mode numbers 0, −1, and +1) are to be used, $\underline{U}$ will be a matrix of order 6×6. The first two rows contain the matching conditions for the electric and magnetic components with the k_x of the zeroth-order mode, the next two the −1 mode, and the last two will contain the +1-mode components. The columns contain the fields in these categories for the 0, −1, and +1 modes forward and backward. For the lth layer, $\underline{U}$ becomes

within the period of the grating, and a similar expression is simultaneously true for the magnetic field.

When calculating the layer matrix that involves the interface between a grating layer and a homogeneous layer, it is necessary to distinguish the cases of (a) a "real" and (b) a perfectly conducting grating, since for a perfect conductor it is incorrect to apply the boundary condition that H_y is conserved for all x across the period. This boundary condition is derived from Ampère's law by calculating the current enclosed by an infinitesimal loop that intersects the surface. If the loop encloses no current as its width is reduced to zero, H_y must be conserved. For a perfector conductor, however, the current driven by the electric field associated with the electromagnetic radiation must be a surface current, and Δz can never be made sufficiently small for the condition to apply. This case is considered later in (b). The boundary condition on E_x, (17), however, is valid for both cases.

1. "Real" gratings

In order to calculate the layer matrix, $\underline{a}_l$ and $\underline{b}_l$ are required in terms of $\underline{a}_g$ and $\underline{b}_g$ in a form independent of x. The solution follows using the standard techniques of Fourier analysis: both sides of (17) are multiplied by the complex conjugate of a Fourier component and integrated over a period to eliminate the summation on the left-hand side and remove the x dependence from both sides. Consider the transformation of the left-hand side using the jth Fourier component, which has $k_x^j = k_{0x} + 2\pi j/d$, and gives, subject to normalization,

$$\int_{\text{one period}} e^{-ik_x^j x} \sum_n [(a_l^n e^{ik_z^n(l)h_l} + b_l^n) e^{ik_x^n x}]dx = a_l^j e^{ik_z^j(l)h_l} + b_l^j . \quad (18)$$

The same procedure may be applied to the right-hand side of (17), which contains the grating eigenmodes, giving

$$\int_{\text{one period}} e^{-ik_x^j x} \sum_m [a_g^m E_g^{m(+)}(x) + b_g^m E_g^{m(-)}(x) e^{-ik_z^m(g)h_g}]dx = \sum_m \left[a_g^m \int_{x=0}^{d} E_g^{m(+)}(x) e^{-ik_x^j x} dx + b_g^m e^{-ik_z^m(g)h_g} \int_{x=0}^{d} E_g^{m(-)}(x) e^{-ik_x^j x} dx \right] . \quad (19)$$

Equations (18) and (19) may be expressed in matrix form reproducing the exact form of the boundary condition for homogeneous layers, Eq. (7). Consider first (18), which is the Fourier transform of the left-hand side of (17). In matrix form, this may be written for the 0, -1, and $+1$ Fourier components simultaneously as

$$\underline{U}_l \underline{K}_l^+ \begin{bmatrix} a_l^0 \\ a_l^{-1} \\ a_l^{+1} \\ b_1^0 \\ b_1^{-1} \\ b_l^{+1} \end{bmatrix} ,$$

where

$$\underline{U}_l = \begin{bmatrix} E_l^{0(+)} & 0 & 0 & E_l^{0(-)} & 0 & 0 \\ H_l^{0(+)} & 0 & 0 & H_l^{0(-)} & 0 & 0 \\ 0 & E_l^{-1(+)} & 0 & 0 & E_l^{-1(-)} & 0 \\ 0 & H_l^{-1(+)} & 0 & 0 & H_l^{-1(-)} & 0 \\ 0 & 0 & E_l^{+1(+)} & 0 & 0 & E_l^{+1(-)} \\ 0 & 0 & H_l^{+1(+)} & 0 & 0 & H_l^{+1(-)} \end{bmatrix} \quad (20)$$

and

$$\underline{K}_l^+ = \begin{bmatrix} e^{ik_z^0(l)h_l} & 0 & 0 & 0 & 0 & 0 \\ 0 & e^{ik_z^{-1}(l)h_l} & 0 & 0 & 0 & 0 \\ 0 & 0 & e^{ik_z^{+1}(l)h_l} & 0 & 0 & 0 \\ 0 & 0 & 0 & 1 & 0 & 0 \\ 0 & 0 & 0 & 0 & 1 & 0 \\ 0 & 0 & 0 & 0 & 0 & 1 \end{bmatrix} .$$

Note that $\underline{U}_l$ in (20) is the same as that in (16) for the ambient layer because the homogeneous-layer modes are identical to the Fourier components used in (18).

Examining (19), it is apparent that no element of the equivalent matrix for the grating layer $\underline{U}_g$ is necessarily zero. This expression can be written in matrix form, keeping to the same conventions, so that each row of the resulting vector is the total field contributing to a particular Fourier component, giving

$$\underline{U}_g = \begin{bmatrix} E^{0(+),0} & E^{1(+),0} & E^{2(+),0} & E^{0(-),0} & E^{1(-),0} & E^{2(-),0} \\ H^{0(+),0} & H^{1(+),0} & H^{2(+),0} & H^{0(-),0} & H^{1(-),0} & H^{2(-),0} \\ E^{0(+),-1} & E^{1(+),-1} & E^{2(+),-1} & E^{0(-),-1} & E^{1(-),-1} & E^{2(-),-1} \\ H^{0(+),-1} & H^{1(+),-1} & H^{2(+),-1} & H^{0(-),-1} & H^{1(-),-1} & H^{2(-),-1} \\ E^{0(+),+1} & E^{1(+),+1} & E^{2(+),+1} & E^{0(-),+1} & E^{1(-),+1} & E^{2(-),+1} \\ H^{0(+),+1} & H^{1(+),+1} & H^{2(+),+1} & H^{0(-),+1} & H^{1(-),+1} & H^{2(-),+1} \end{bmatrix}, \tag{21}$$

where the first superscript on $E^{m(\pm),n}$ determines which grating eigenmode is involved in the term, and the second identifies the homogeneous-layer eigenmode:

$$E^{m(\pm),n} = \frac{1}{d}\int_{x=0}^{d} E_g^{m(\pm)}(x) e^{-ik_x^n x} dx \ . \tag{22}$$

The same algorithm that has been applied to the layer matrix between homogeneous layers will now generate an equivalent matrix for the interface between a homogeneous layer and a grating.

2. *Perfectly conducting gratings*

It has already been noted that the full layer matrix in the case of a perfectly conducting grating cannot be found using the boundary conditions that were applied to the "real" grating. The continuity condition still applies to the electric field, but no longer applies to the magnetic field across the whole period.

The equivalent of (17) for the magnetic field is

$$\sum_n [(a_l^n H_l^{n(+)} e^{ik_z^n(l) h_l} + b_l^n H_l^{n(-)}) e^{ik_x^n x}]$$
$$= \sum_m [a_g^m H_g^{m(+)}(x) + b_g^m H_g^{m(-)}(x) e^{-ik_z^n(g) h_g}] \ . \tag{23}$$

Equation (23) is valid only in the "gap" region of the grating, since this is the only region in which H_y must be continuous, so the integrals in (19) may now be applied only over this interval. Since the field of the grating mode in the finger region is zero, no change (other than the normalization of the integral) is needed to the overlap integral in the grating eigenmode matrix, which therefore retains the form of (21). On the other hand, the homogeneous-layer eigenmode matrix (20) must be modified to

$$\underline{U}_l = \begin{bmatrix} E_l^{0(+)} & 0 & 0 & E_l^{0(-)} & 0 & 0 \\ H_l^{0(+),0} & H_l^{-1(+),0} & H_l^{+1(+),0} & H_l^{0(-),0} & H_l^{-1(-),0} & H_l^{+1(-),0} \\ 0 & E_l^{-1(+)} & 0 & 0 & E_l^{-1(-)} & 0 \\ H_l^{0(+),-1} & H_l^{-1(+),-1} & H_l^{0(+),-1} & H_l^{0(-),-1} & H_l^{-1(-),-1} & H_l^{+1(-),-1} \\ 0 & 0 & E_l^{+1(+)} & 0 & 0 & E_l^{+1(-)} \\ H_l^{0(+),+1} & H_l^{0(+),+1} & H_l^{+1(+),+1} & H_l^{0(-),+1} & H_l^{-1(-),+1} & H_l^{+1(-),+1} \end{bmatrix}, \tag{24}$$

where

$$H_l^{m(\pm),n} = \frac{1}{(1-r)d}\int_{rd/2}^{(1-r/2)d} H_l^{m(\pm)}(x) e^{-ik_x^n x} dx \ . \tag{25}$$

Note that this integral differs from those in (22), as it involves the overlap of one homogeneous-layer mode with another in a limited region of the period rather than the overlap of a homogeneous-layer mode with a grating mode across the whole period.

In the next section, it is shown how the scattering matrix is used to calculate the optical response of the system: not only the reflection and transmission coefficients for all the diffracted beams, but the amplitudes of the fields throughout the entire system and the dispersion relations of localized modes in the system may be found.

D. Quantities derived from the scattering matrix

1. *Reflection and transmission coefficients*

Most experiments that measure reflection and transmission coefficients in fact record the time-averaged power coefficients R and T, which are related to the amplitude coefficients r and t by $R = rr^*$ and $T = tt^*$. In a system with a diffraction grating, the notation must be extended to distinguish the various grating orders, thus t^{ij} will be used to represent the ratio of the amplitudes of

the transmitted jth mode to the incident ith mode:

$$t^{ij}=\frac{E_{L+1}^{j(+)}}{E_0^{i(+)}} , \tag{26}$$

where the $(\pm)$ symbol indicates direction of propagation and the subscripts 0 and $L+1$ are the layer indices. The electric fields on the right-hand side of (26) are associated with eigenmodes that are either incident on or scattered by the system, and must therefore be related by an appropriate element of the scattering matrix for the whole system, $S^{i(+),j(+)}$. For simplicity, this element will be referred to as s, satisfying $E_x^{j(+)}(L+1)=sE_x^{i(+)}(0)$. The power transmission coefficient is then given by

$$|s|^2\frac{\mathrm{Re}[k_z^i(0)]}{\mathrm{Re}[k_z^j(L+1)]}\frac{\mathrm{Re}[\epsilon(L+1)]}{\mathrm{Re}[\epsilon(0)]} \tag{27}$$

where the additional factor corrects for the different dielectric constants of the ambient and substrate media and the different directions of propagation. Similar expressions apply for the reflected modes and for both transmitted and reflected modes in the case of s polarization.

2. EM field profiles

The electric and magnetic fields can be found at any point in the system, provided that the mode coefficients $\underline{a}_l$ and $\underline{b}_l$ are known. These may be found using the scattering matrices $\underline{S}(0,l)$ for the partial system up to layer l, which are found in the course of the construction of the scattering matrix for the entire structure $\underline{S}(0,L+1)$.

Assuming the coefficients of the incident eigenmodes $\underline{a}_0$ are known and that there are no modes incident upon the system from the substrate layer ($\underline{b}_{L+1}=\underline{0}$), the eigenmodes scattered from the entire system may be found from the definition of the scattering matrix:

$$\begin{bmatrix}\underline{a}_{L+1}\\ \underline{b}_0\end{bmatrix}=\underline{S}(0,L+1)\begin{bmatrix}\underline{a}_0\\ \underline{b}_{L+1}\end{bmatrix} . \tag{28}$$

$\underline{b}_0$ may be determined fom this equation, and then the coefficients of the eigenmodes in any layer l may be found by solving

$$\begin{bmatrix}\underline{a}_l\\ \underline{b}_0\end{bmatrix}=\underline{S}(0,l)\begin{bmatrix}\underline{a}_0\\ \underline{b}_l\end{bmatrix} \tag{29}$$

for $\underline{a}_l$ and $\underline{b}_l$. The solution is

$$\begin{aligned}\underline{b}_l&=\underline{S}_{22}^{-1}(\underline{b}_0-\underline{S}_{21}\underline{a}_0) ,\\ \underline{a}_l&=\underline{S}_{11}\underline{a}_0+\underline{S}_{21}\underline{b}_l ,\end{aligned} \tag{30}$$

where the subscripts on $\underline{S}$ refer to the four "quarter" submatrices as defined in Sec. II.

The elements of the vectors $\underline{a}_l$ and $\underline{b}_l$ give the amplitudes of the components of the fields associated with the eigenvectors in each layer (E_x and H_y for p polarization). The eigenmodes propagate as plane waves with known k_x and k_z in each homogeneous layer, so the fields at any point in the homogeneous layers are easily found. For example, the total E_x field in layer l $[Z(l-1)<z<Z(l)]$ is given by

$$E_x(x,z)=\sum_n(a_l^n e^{ik_z^{n(+)}[z-Z(l-1)]}+b_l^n e^{ik_z^{n(-)}[z-Z(l)]})e^{ik_x^n x} . \tag{31}$$

The other components of the fields may be found by applying Maxwell's equations and using expressions analogous to (27).

The fields may be found within the grating layer because the x dependence of the eigenmodes is known. This dependence replaces the $e^{ik_x^n x}$ term on the right-hand side of (31), but the z dependence of the eigenmodes remains $e^{ik_z^n z}$.

3. Dispersion relations

The scattering matrix also provides a relatively simple means to determine the dispersion relation of the electromagnetic eigenmodes of the complete system. This dispersion relation is the set of combinations of k_x and ω for which the system supports finite-amplitude modes decaying into the ambient and substrate layers in the absence of incident modes. This implies that

$$\begin{bmatrix}\underline{a}_{L+1}\\ \underline{b}_0\end{bmatrix}=\underline{S}(0,L+1)\begin{bmatrix}\underline{0}\\ \underline{0}\end{bmatrix} \tag{32}$$

with nonzero $\underline{a}_{L+1}$ and $\underline{b}_0$. For this to be true, the determinant of the inverse of the scattering matrix must be zero:

$$f(k_x,\omega)=\det\underline{S}^{-1}(0,L+1)=0 . \tag{33}$$

In general, this will only be satisfied if one of k_x and ω is allowed to be complex. For example, if k_x is taken to be real (representing a system eigenmode that translationally invariant along the x axis), an imaginary part of ω represents the decay of the mode with time.

$f(k_x,\omega)$ is a complex function, and it is possible to search for the complex roots of (33) using one of several suitable techniques described in Ref. 11. Determining the roots of (33) can be very difficult, because the determinant is a rather badly behaved function in that it has many local minima and maxima that root-finding algorithms find hard to distinguish from zeros and poles. However, the correct root can also be found by searching for poles of the individual elements of the scattering matrix.

In fact, finding the poles of the individual elements of $\underline{S}$ can yield more useful information than the determinant method, because only those system eigenmodes that have field distributions corresponding to the element chosen will be found. For example, consider the case of a system with a grating of period d. The grating will cause a system eigenmode to be zone folded with a "Brillouin-zone" boundary at π/d, as shown in Fig. 4. Finding the zeros of $\det\underline{S}^{-1}$ should determine all the branches of the dispersion relation, whereas finding the poles of an ele-

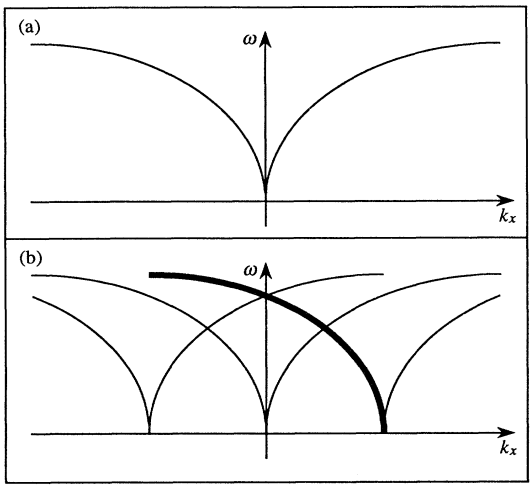

FIG. 4. Hypothetical zone-folded dispersion relation shown without the zone folding in (a) and in the periodic zone scheme in (b). Only a single branch (such as the one that is highlighted in this figure) is picked out by finding the poles of a single element of the scattering matrix.

ment would be more selective. For example, if k_x is varied in the range $-\pi/d < k_x < \pi/d$, searching for poles in the element that gives the reflected amplitude of the eigenmode with $k_x = k_{0x} + 2\pi/d$ would find only the highlighted branch in Fig. 4. This branch is the system eigenmode that has been shifted by $2\pi/d$ by the presence of the grating.

In many systems with complicated dispersion relations, interacting branches do not cross but repel each other, and in these cases, it can sometimes be difficult to assign physical meaning to the different branches. Apart from the comparative ease with which roots can be found, the advantage of finding the poles of a particular element rather than the determinant of $\underline{S}^{-1}$ is that the branches picked out will have the same physical character, determined by the choice of element. By searching for poles of different elements, the physical character of each branch of the dispersion relation can be identified.

IV. APPLICATIONS OF THE SCATTERING MATRIX

A. Grating coupling to surface plasmons at visible wavelengths

The introduction of a grating greatly increases the complexity of the calculation of the optical response of a system, and thus increases the difficulty of verifying the results. However, there are several tests that can be applied to the results of the scattering-matrix method. The visible frequency range is particularly attractive for confirming the validity of the method because of the ease with which predictions can be tested experimentally. Furthermore, the visible frequency range offers a more stringent test than the far infrared because the wavelength can be made comparable to the grating period, and thus the number of diffracted orders that transport energy away from the grating can be varied.

1. The results of Sheng et al.

As a preliminary test, the results obtained using the scattering-matrix method can be compared with those obtained by Sheng, Stepleman, and Sanda[7] using a transfer-matrix approach. In Ref. 7, the reflectivity of a lamellar silver grating ($d = 1$ μm, $h_g = 60$ nm, $r = 0.34$) on a silver substrate was calculated at a wavelength of 647.1 nm and for a range of angles of incidence. The calculation was found to be in good agreement with an experiment conducted using a Kr laser source.

The same system has now been modeled using identical parameters with the scattering-matrix method, and the result is presented in Fig. 5. The agreement with Sheng's result is very good, indicating that the scattering-matrix method is stable and has been implemented correctly. The dashed line gives the sum of the power reflected in all the diffracted orders of the grating, R_{tot}, and illustrates that two distinct physical processes combine to produce the line shape of the specular (zeroth-order) reflectance R_0. The large absorption features at 13°, 25°, and 60° that feature in both curves corresponds to the excitation of surface-plasmon polaritons (SPP's), and represent a transfer of energy from free electromagnetic radiation to surface modes. The broad trough between 17° and 24° in the zeroth-order reflectance does not feature in the total reflectance, and corresponds to a redistribution of the propagating energy between the various diffraction orders as the higher orders appear or disappear over the "horizon." Clearly the total energy in the modes should add up to nearly unity ($R_{\text{tot}} \sim 1$), as is apparent in Fig. 5, because silver is a good conductor and

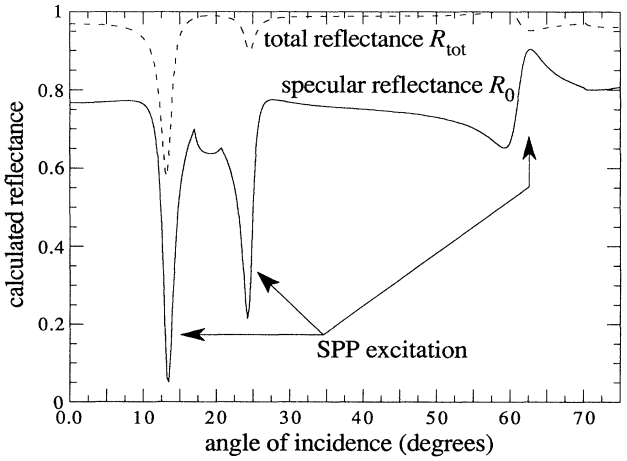

FIG. 5. Scattering-matrix calculation of reflectance from a silver grating ($d = 1$ μm, $r = 0.34$, $h_g = 60$ nm) on a silver substrate at a wavelength of 647.1 nm. The result is indistinguishable from that obtained by Sheng, Stepleman, and Sanda (Ref. 7) using a transfer-matrix approach, but the scattering-matrix method allows the inclusion of multilayer substrates.

little energy is lost in driving surface currents on reflection.

2. Convergence

The result of the scattering-matrix calculation for systems with lamellar gratings will clearly depend on the number of eigenmodes included in the calculation. The reflection spectrum shown in Fig. 5 was calculated including a total of 17 diffracted orders ($M=17$, matrices of order $2M\times 2M$). For $M>17$, the variation in calculated transmission was less than 1%, even at the surface-plasmon resonances.

3. Field matching at boundaries

In order to confirm that the x component of the electric field is conserved across the grating-layer–homogeneous-layer interface, the E_x profiles have been calculated on each side of the interface and the fractional difference calculated as a function of x. Figure 6 shows (on a logarithmic scale) the comparison between $|E_x|^2$ calculated just inside the grating and in the ambient at the same interface for $M=17$. The match between the fields of the grating and the fields of the homogeneous layer shown in Fig. 6 is as good as could be expected given the number of Fourier terms retained in the expansion of the homogeneous fields ($M=17$ requires homogeneous layer modes in the range -8–$+8$). The conclusion is therefore that this implementation of the scattering-matrix calculation satisfies the field matching requirements.

4. Energy conservation

If the scattering-matrix calculation is correct, the calculated electromagnetic response of the system must satisfy the requirement of conservation of energy. In the discussion of the calculated reflectivities shown in Fig. 5, it was noted that the total reflectance R_{tot} was close to unity except at the surface-plasmon resonances. If the silver grating is replaced by a perfectly conducting grating and the absorption in the substrate (i.e., the imaginary part of the dielectric constant) is set to zero, an absorption-free system is obtained, in which the total reflectivity must be exactly unity. The calculated angular dependence of the reflectance for this system at wavelength 647.1 nm is shown in Fig. 7.

The general form of R_0 is the same as in Fig. 5, but now the minima at the SPP resonances go to zero and have been shifted slightly, primarily because of the change in the nature of the surface. However, in contrast to Fig. 5, here there are no absorption features in R_{tot}. The sharp troughs in R_0 corresponding to SPP excitation are still present, but the energy that was absorbed from the zeroth order by this excitation in the lossy system is now totally reradiated in other orders. R_{tot} is thus very close to unity, as expected, except for angles of incidence greater than about 65°, indicating, perhaps, that convergence has not quite been achieved there. In fact, the -3-order diffracted beam appears over the "horizon" at 70°, so it is reasonable that more eigenvalues are needed for $\theta>70°$ than for $\theta<70°$. Other than in this region, though, it is apparent that the energy-conservation requirement is satisfied by the scattering-matrix calculation for this system.

B. Gratings in the far-infrared range

In the far-infrared range (FIR), metal gratings can be modeled using the eigenmodes of a perfectly conducting grating, because the skin depth for a real metal is much less than the grating period. One of the most important uses of a grating in the FIR is to act as an optical

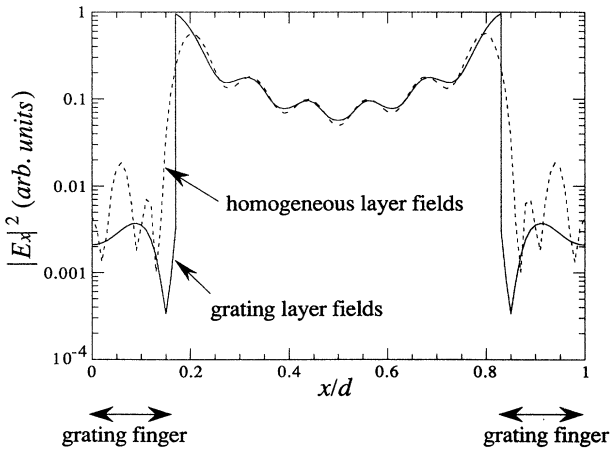

FIG. 6. Field matching at the grating–substrate interface for the calculation in Fig. 5 at normal incidence. The fields of the eigenmodes of both layers penetrate the grating metal to some extent, but there is a sharper discontinuity in the grating layer field profile. Nevertheless, the fields are well matched across the entire grating period. (Note that the field strength is plotted on a logarithmic scale.)

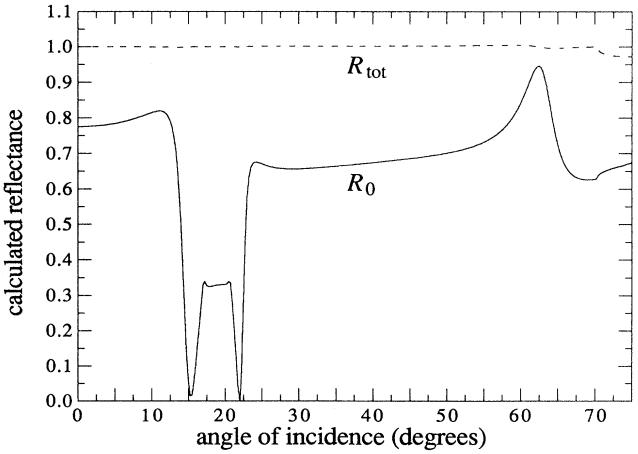

FIG. 7. Scattering-matrix calculation for the same grating-substrate as was used for Fig. 5, but with the silver grating replaced by a perfect conductor and the absorption in the silver substrate set to zero, removing any absorption. In this case, energy can be seen to be conserved because $R_{\text{tot}}=1$.

coupler,[12] allowing the nonradiative two-dimensional plasmon resonance to interact with freely propagating FIR radiation. This process is investigated in this section for a two-dimensional electron gas (2DEG) at an $Al_{1-x}Ga_xAs/GaAs$ heterojunction.

1. Modeling a 2DEG

A 2DEG may be included in the calculation as an infinitely thin conducting sheet at the interface between two "normal" layers in the calculation. The sheet is then modeled through its conductivity, which allows the sophistication of the model of the 2DEG to be increased very easily. In this case, the concept of eigenmodes in the sense used during the derivation of the scattering-matrix method in Sec. II has no meaning. The effect of the 2DEG is to change the boundary conditions relating the fields in the two adjacent layers rather than to act as an independent layer in its own right. In particular, the electric field E_x (for p polarization), which is conserved across the interface, drives a surface current $j_x(\omega)=\sigma(\omega)E_x(\omega)$. This current determines the difference in H_y across the 2DEG (which is taken as separating layers l and $l+1$) according to the usual electromagnetic boundary conditions:

$$H_y(l)=H_y(l+1)+j_x$$
$$=H_y(l+1)+\sigma_{xx}(\omega)E_x(l+1)\ . \tag{34}$$

The condition that $H_y(l)=H_y(l+1)$, which was implicit in the calculation of the layer matrix in (7), is thus no longer valid; however, the same calculation can be used if the appropriate elements of $\underline{U}_{l+1}$ in (9) are modified to include the σE_x term.

The calculations presented below were made for the system illustrated in Fig. 8. The substrate and the thin layer of $Al_{1-x}Ga_xAs$ (typically $h_{Al_{1-x}Ga_xAs}\approx 700$ Å) that separates the 2DEG from the grating were modeled as plasmon-phonon systems using the dielectric function

$$\epsilon(\omega)=\epsilon_\infty+\frac{f\omega_{TO}^2}{\omega_{TO}^2-\omega^2-i\Gamma\omega}-\frac{\epsilon_\infty\omega_p^2}{\omega^2+i\omega/\tau}\ ,$$

where f is the phonon oscillator strength, ω_{TO} and Γ are the TO phonon frequency and scattering parameter, respectively, ω_p and τ are the 3D plasmon frequency and Drude relaxation time, respectively, and ϵ_∞ is the high-frequency relative dielectric constant. These parameters are available for GaAs and $Al_{1-x}Ga_xAs$ in the literature.[13]

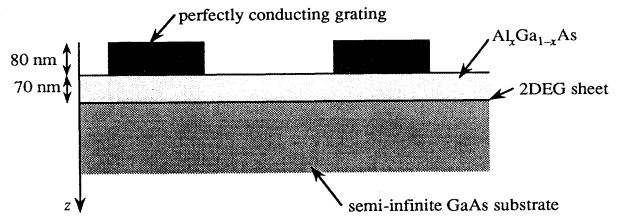

FIG. 8. The model of a heterojunction 2DEG system used for the FIR calculations. The grating period was $d=1$ μm and the mark fraction $r=0.33$.

2. Transmission and reflection

A typical calculated FIR transmission spectrum is shown in Fig. 9. The transmission is found for two values of the 2DEG charge density, in this case $N_S=0$ and 3.5×10^{11} cm^{-2} and the fractional difference

$$-\frac{\Delta T}{T}=\frac{T(N_S=0)-T(N_S=3.5\times10^{11}\ \text{cm}^{-2})}{T(N_S=0)}$$

is plotted as a function of frequency. This normalization procedure removes the background absorption associated with the substrate material, and leaves only those features that are caused by the 2DEG.

The principal features of the transmission spectrum are an increasing absorption to low frequency, the Drude absorption, and the first- and second-order plasmon resonances at 34 and 49 cm^{-1}. Figure 9 is in good qualitative agreement with optical experiments in the literature; see, e.g., Ref.12.

No experimental reflectance studies of this kind of structure have been reported in the literature, so an experiment has been carried out using a Bruker IFS 113v FIR Fourier-transform spectrometer. A molecular-beam-epitaxy (MBE)-grown $Al_{1-x}Ga_xAs/GaAs$ heterojunction system with an overlaid Al grating of period 1 μm and mark fraction 0.33 prepared by electron-beam lithography was cooled to 4.2 K, and the reflectance was measured using a liquid-helium-cooled silicon bolometric detector. The charge density in the sample was varied by applying a bias voltage V_g between the 2DEG and the overlaid metallic grating. The result,

$$+\frac{\Delta R}{R}=\frac{R(V_g=0\ V)-R(V_g=+0.2\ V)}{R(V_g=+0.2\ \text{V})}\ ,$$

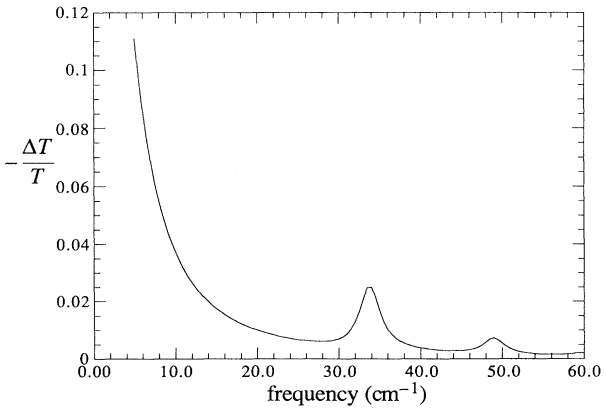

FIG. 9. Calculated change in FIR transmission through the sample illustrated in Fig. 8 caused by the presence of the 2DEG. The first- and second-order two-dimensional plasmon-absorption peaks can be seen at 34 and 49 cm^{-1}. The large increase in absorption at low frequency is the Drude absorption tail.

is plotted in Fig. 10. The plasmon resonance from the $V_g = 0$ V spectrum is evident as a positive-going feature at 28 cm^{-1}, and that from $V_g = +0.2$ V is a negative-going peak at 31 cm^{-1}; the plasmon resonance is seen as an *increase* in reflectance rather than a decrease, as in transmission. Further experimental details will be published separately.[14]

The scattering-matrix method is readily capable of calculating the fractional difference in reflectance, and the experimental system has been modeled using the parameters in Fig. 8, giving a good agreement with the experimental data for

$$+\frac{\Delta R}{R} = \frac{R(N_S = 2.4\times 10^{11}\ \text{cm}^{-2}) - R(N_S = 2.8\times 10^{11}\ \text{cm}^{-2})}{R(N_S = 2.8\times 10^{11}\ \text{cm}^{-2})} .$$

The result of this calculation is shown in Fig. 11, and confirms that the scattering-matrix calculation is in excellent agreement with experimental data for plasmon spectroscopy.

3. *Field profiles*

It is well known that the optical excitation of a surface-plasmon resonance at a metal-dielectric interface is accompanied by a large increase in the electric-field strength close to the interface.[15] However, no similar investigations have been made for two-dimensional plasmons. In Fig. 12, the x component of the electric field at the 2DEG is plotted over one grating period at the first- and second-order plasmon resonances and at another frequency away from these resonances. It is immediately clear that a strong field enhancement does occur at the plasmon resonances.

4. *Dispersion relations*

Figure 13 shows two calculations of the 2D plasmon dispersion relation for a heterojunction 2DEG system. In (a), a grating has not been placed over the sample surface, and the expected approximate square-root dependence of ω on k is apparent. In (b), a perfectly conducting grating has been added to the system, and the dispersion relation is now zone folded and gaps have opened at integral multiples of π/d. The expected plasmon dispersion relation is[16]

$$\omega^2 = \frac{N_S e^2 k_x}{2m^* \epsilon_0 \bar{\epsilon}} , \tag{35}$$

where $\bar{\epsilon}$ includes the screening effect of the gate. For the cases of a continuous perfectly conducting gate (closed surface) and a vacuum interface (open surface), $\bar{\epsilon}$ is given by

$$\bar{\epsilon} = \frac{\epsilon_{\text{GaAs}} + \epsilon_{\text{Al}_{1-x}\text{Ga}_x\text{As}} \coth(k_x h_{\text{Al}_{1-x}\text{Ga}_x\text{As}})}{2} \tag{36}$$

for a closed surface,[17] and

$$\bar{\epsilon} = \frac{\epsilon_{\text{GaAs}} + \epsilon_{\text{Al}_{1-x}\text{Ga}_x\text{As}} \tanh(k_x h_{\text{Al}_{1-x}\text{Ga}_x\text{As}})}{2} \tag{37}$$

for an open surface,[18] where ϵ_{GaAs} and $\epsilon_{\text{Al}_{1-x}\text{Ga}_x\text{As}}$ are the dielectric constants of GaAs and $Al_{1-x}Ga_xAs$ and $h_{\text{Al}_{1-x}\text{Ga}_x\text{As}}$ is the thickness of the $Al_{1-x}Ga_xAs$ layer. These formulas will be referred to as the "coth" and "tanh" formulas, respectively.

The tanh formula agrees well with the scattering ma-

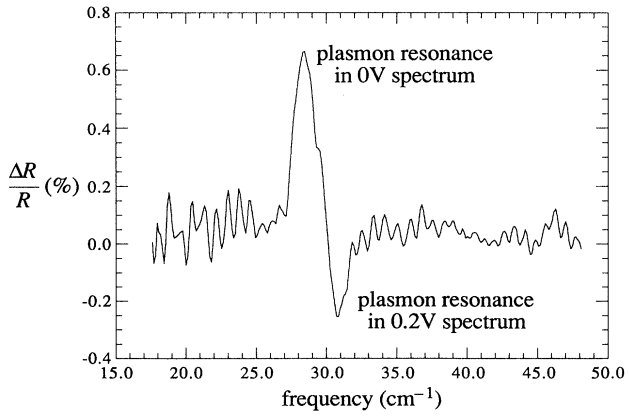

FIG. 10. Experimental fractional change in reflectance for a heterojunction sample under a small change in grating-gate bias. Plasmon resonance is indicated by an increase in reflectance.

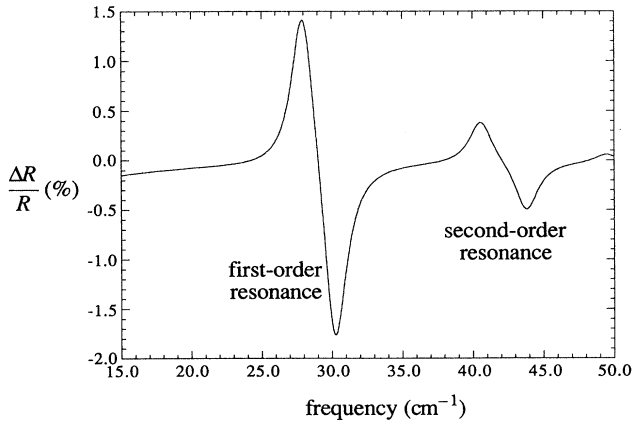

FIG. 11. Calculated fractional change in reflectance for the sample for which the experimental data in Fig. 10 was collected. In agreement with the experimental data, the plasmon resonance is marked by an increase in reflection. In the calculation, the second-order plasmon resonance can also be seen, although it was not resolved in the experimental data.

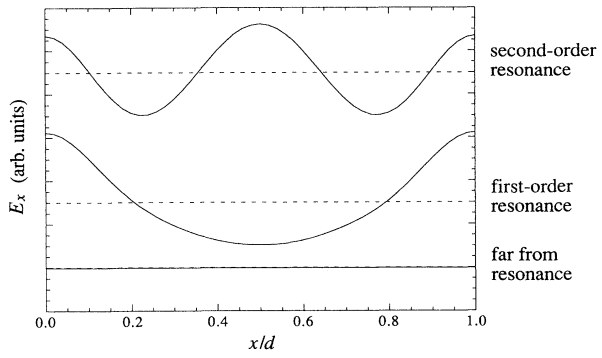

FIG. 12. E_x field profiles across one period of the grating at the first- and second-order plasmon resonances and away from these resonances. Note that the field amplitude is enhanced at resonance by several orders of magnitude. The gap between fingers of the grating gate occupies the region $0.17 < x/d < 0.83$, and some enhancement of the field under the fingers is apparent for the first-order resonance.

trix calculation for an ungated heterojunction in Fig. 13(a), as expected, but neither of these formulas gives a good agreement for the calculation with a grating gate in Fig. 13(b). The screening in this system is clearly intermediate between the extreme cases for which (36) and (37) are applicable, and this is reflected in that the plasmon frequency is intermediate between those predicted using these formulas. A more detailed investigation of the dispersion relation in a grating-gated heterojunction will be presented in another publication.[19]

V. CONCLUSIONS

The scattering-matrix method provides a useful formalism for the calculation of the optical response of stratified systems. The method has been extended here to allow the inclusion of lamellar gratings, and yields the reflection and transmission coefficients for all the diffracted orders, the electromagnetic-field distributions, and the dispersion relations of any localized eigenmodes supported by the system. These algorithms may be used together to establish a clear physical understanding of the electromagnetic response of a wide range of systems. The reflection and transmission coefficients allowed a comparison to be made between the calculations and experimental data. If the dispersion relations are found, any observed resonances may be identified as corresponding to a particular excitation of the system. The field profiles may then be examined to provide unambiguous confirmation of the physical nature of that excitation.

The calculations described in this paper are relatively easily implemented and can be performed on desktop workstations, without the need for supercomputer resources. The results are in excellent agreement with experiment and other theoretical approaches, and the method is expected to be widely applicable in the frequency range from the far infrared to the visible. The EM properties of a layer may be altered without changing the method of calculation, and it is expected that the method will prove useful in the study of many-layered systems, such as thin magnetic films (the magneto-optical Kerr effect) and liquid-crystal systems.

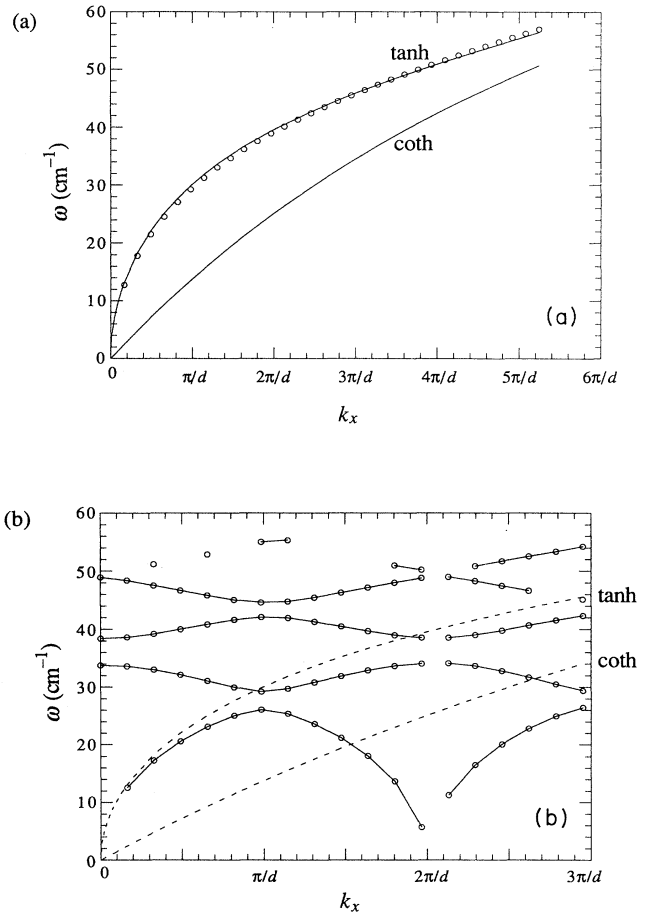

FIG. 13. (a) Dispersion relation for a two-dimensional plasmon in an ungated semiconductor heterojunction system. (b) Dispersion relation for a two-dimensional plasmon in a grating-gated heterojunction system. Note that the dispersion is zone folded and gaps have opened at the zone boundaries. The curves labelled "coth" and "tanh" apply to heterojunctions with a continuous perfectly conducting gate and an open surface, respectively. The grating-gated case clearly falls in between these two extremes.

ACKNOWLEDGMENTS

Gratings were fabricated by D. G. Hasko and H. Ahmed (MRL, Cambridge, UK), on heterostructure samples provided by J. E. F. Frost, D. C. Peacock, D. A. Ritchie, and G. A. C. Jones (Cavendish Laboratory, Cambridge, UK) and C. R. Whitehouse and N. Apsley (RSRE, Malvern, UK). The FIR reflection data were measured by R. J. Wilkinson. C.D.A. would like to thank the SERC, Trinity College and St. John's College, Cambridge, UK for financial support.

[1]F. Abèles, Ann. Phys. (Paris) **5**, 596 (1950); **5**, 702 (1950).
[2]S. Teitler and B. W. Henvis, J. Opt. Soc. Am. **60**, 830 (1970).
[3]D. W. Berreman, J. Opt. Soc. Am. **62**, 502 (1972).
[4]D. Y. K. Ko and J. C. Inkson, Phys. Rev. B **38**, 9945 (1988); D. Y. K. Ko and J. R. Sambles, J. Opt. Soc. Am. **5**, 1863 (1988).
[5]W. C. Chew, *Waves and Fields in Inhomogeneous Media* (Van Nostrand Reinhold, New York, 1990), pp. 136–140.
[6]R. Petit, in *Electromagnetic Theory of Gratings,* edited by R. Petit, Springer Topics in Modern Physics Vol. **22** (Springer, Heidelberg, 1980), pp. 1–52.
[7]Ping Sheng, R. S. Stepleman, and P. N. Sanda, Phys. Rev. B **26**, 2907 (1982).
[8]J. L. Uretski, Ann. Phys. **33**, 400 (1965); A. Wirgin, Rev. Opt. **9**, 449 (1964).
[9]Xu Shanjia and Wu Xinzhang, Int. J. Infrared Millimeter Waves **11**, 1047 (1990).
[10]A. Yariv and P. Yeh, *Optical Waves in Crystals* (Wiley, New York, 1984), p. 167.
[11]W. H. Press, B. P. Flannery, S. A. Teukolsky, and W. T. Vettering, *Numerical Recipies* (Cambridge University Press, London, 1986).
[12]S. J. Allen, Jr., D. C. Tsui, and F. DeRosa, Phys. Rev. Lett. **35**, 1359 (1975).
[13]K. A. Maslin, T. J. Parker, N. Raj, D. R. Tilley, P. J. Dobson, D. Hilton, and C. T. B. Foxon, Solid State Commun. **60**, 461 (1986).
[14]R. J. Wilkinson, C. D. Ager, T. Duffield, H. P. Hughes, D. G. Hasko, H. Ahmed, J. E. F. Frost, D. C. Peacock, D. A. Ritchie, G. A. C. Jones, expected C. R. Whitehouse, and N. Apsley (unpublished).
[15]E. Kretschmann, Z. Phys. **241**, 313 (1971).
[16]F. Stern, Phys. Rev. Lett. **18**, 546 (1967).
[17]A. V. Chaplik, Zh. Eksp. Teor. Fiz. **62**, 746 (1972) [Sov. Phys.—JETP **35**, 395 (1972)].
[18]N. Okisu, Y. Sambe, and T. Kobayashi, Appl. Phys. Lett. **48**, 776 (1986).
[19]C. D. Ager, R. J. Wilkinson, and H. P. Hughes, J. Appl. Phys. (to be published).